Evaluation of accelerometers to determine pavement deflections under traffic loads

Materials and Structures (2009) 42:779–790
DOI 10.1617/s11527-008-9423-5

ORIGINAL ARTICLE

Evaluation of accelerometers to determine pavement deflections under traffic loads

M. Arraigada · M. N. Partl · S. M. Angelone · F. Martinez

Received: 2 November 2007 / Accepted: 21 August 2008 / Published online: 30 August 2008

Abstract The purpose of this work was to study the use of accelerometers to measure pavement deflections due to traffic loads. To this end, accelerometers were embedded in two sites: the full scale load simulator Circular Test Track (CTT) and the A1 motorway in Switzerland. Deflections were derived from acceleration measurements using an algorithm that double integrates the measured signal and corrects any errors derived from the procedure. In the motorway, deflections were monitored using a set of three magnetostrictive deflectometers. Additionally, the pavement's material viscoelastic parameters determined in the laboratory were incorporated in Finite Element (FE) models to estimate the theoretical deflections. The calculated deflections were then compared to the measured and to the theoretical deflections. Deflections calculated from acceleration showed a reasonable qualitative correlation to those measured by magnetostrictive deflectometers. In addition, the FE models revealed the inability of the accelerometers to measure very slow or quasi-static motion.

Keywords Pavement deflections · Accelerometers · Deflectometers · Finite elements · Pavement modelling

M. Arraigada (✉) · M. N. Partl
Road Engineering/Sealing Components, Swiss Federal Laboratories for Materials Testing and Research (EMPA), Ueberlandstrasse 129, Duebendorf CH-8600, Switzerland
e-mail: martin.arraigada@empa.ch

M. N. Partl
e-mail: manfred.partl@empa.ch

M. Arraigada · S. M. Angelone · F. Martinez
Laboratorio Vial—Instituto de Mecánica Aplicada y Estructuras (IMAE), Universidad Nacional de Rosario, Riobamba y Berutti, 2000 Rosario, Argentina

S. M. Angelone
e-mail: sangelon@fceia.unr.edu.ar

F. Martinez
e-mail: fermar@fceia.unr.edu.ar

1 Introduction

The response of a multilayered flexible pavement to the load of a vehicle is complex. The variety of possible geometries, materials, layer interfaces, loads, weather effects, etc. make the prediction of pavement behaviour a challenging task. In order to study the response of the entire structure to traffic loading, monitoring sites are usually instrumented with deflection, strain, pressure, temperature and humidity sensors. Data obtained from in-situ measurements are used to validate and develop theoretical models. Using the models it is possible to predict the response of pavements under different conditions, thus helping to improve design, extend pavement life and reduce maintenance costs.

Deflectometers at different depths such as multi-depth deflectometers with LVDT [1, 2] and magnetostrictive deflection sensors [3] are the most commonly used sensors to measure deflections and differential vertical deformations of pavements under the loads of a vehicle. However, these sensors have two main drawbacks. Firstly, it is only possible to measure displacements relative to a fixed reference point and secondly, due to the necessity of anchoring far below the deflecting pavement, the installation is quite complicated. On the other hand, inertial sensors, i.e. accelerometers, are of small size, measure absolute values and are relatively simple to install. The conversion from accelerations to deflections has, however, its own drawbacks, namely that it introduces errors that need to be studied and quantified. This may be one reason why only few laboratory and field studies comparing performance and use of these sensors are available in the literature [4, 5] clearly demonstrating that further research on this subject is needed.

Thus, the purpose of this work was to compare the deflections obtained from acceleration measurements on the road to those determined with other methods. The main questions to answer were: Do acceleration measurements provide accurately the structural deflection of a pavement under a moving truck? How do the speed and load of the vehicle influence the results? Would it be possible to use multiple accelerometers arrays to obtain deflection maps with relatively low installation effort and cost? Can these results be used to validate structural models and thus to predict the strain–stress situation of a flexible pavement under vehicular load?

To this end, accelerometers were embedded in different asphalt pavements. Next, the structures were loaded with moving tires. Induced deflections were derived from measured accelerations using numerical double integration and a correction method, as explained in the next section. Calculated deflections in one of the testing sites, the A1 motorway, were contrasted to those obtained from magnetostrictive deflectometers installed at the same position. On the other hand, Finite Element (FE) models of the pavements were prepared. Viscoelastic material characteristics were used to model the behaviour of the asphalt concrete layers. First, the materials of the FE models were validated with static tests. Then, the calibrated model was used to simulate the pavement performance under moving tires. Theoretical deflections were compared to those obtained from accelerometers. The model was also utilized to estimate and compare the pavement deflections at another testing site, the Circular Test Track (CTT), were no deflectometers but accelerometers were installed.

2 Methods

In this section, a brief overview of the background theory related to the topics of this paper is presented. First, the problems and the proposed solutions involving the conversion of acceleration into deflections are reviewed. Then, the deduction of linear viscoelastic parameters of asphalt concrete materials from frequency dependent test data, like the Coaxial Shear Tests (CAST) [6] data, is described.

2.1 From acceleration to deflection

In this work, acceleration were measured at different point in the pavement structure and stored in a digital file. As described in [7], deflections can be calculated by numerical double integration of the measured acceleration using the following equations:

$$vc_{(i)} = vc_{(i-1)} + \frac{a_{(i-1)} + a_{(i)}}{2}\Delta t \quad (1)$$

$$dc_{(i)} = dc_{(i-1)} + \frac{vc_{(i-1)} + vc_{(i)}}{2}\Delta t \quad (2)$$

where $a_{(i)}$ is the acceleration value at ith sample; $vc_{(i)}$, the calculated velocity at ith sample; $dc_{(i)}$, the calculated deflection at ith sample.

However, double integration operates like a filter amplifying low frequencies of the original signal. In case of pavement acceleration, it boosts small acceleration baseline offsets (errors or distortions in the measurement's reference level of motion) converting them into unacceptable drifts of the calculated deflection. Hence, a simple and efficient correction method to eliminate the drift was proposed.

The method identifies the drift in the calculated deflection assuming that the deflection is zero when the pavement is motionless, i.e. in the absence of the mechanical load of a tire. This assumption holds true a moment before and after the tire load reaches the measuring position. Between these two moments the drift is unknown, but can be estimated using a spline

interpolation. Experience has shown that linear baseline correction techniques like the one presented in [8] are not suitable to approximate the random drifts obtained after double integration of road accelerations. Hence, an *n*th-order polynomial function is used for this purpose. Subtracting the polynomial function from the calculated deflection then gives the corrected deflection.

For the automatic calculation of the real deflection, a computer algorithm was written. The algorithm integrates the digital acceleration signal and implements the correction as explained before. To this end, the algorithm detects in the acceleration file the moment where a tire is applying a load near the measuring point defining a threshold value and calculating the sliding root mean square (rms) of the acceleration signal with the following equation:

$$\overline{a}_{\left(\frac{n+i}{2}\right)} = \sqrt{\frac{\sum_{i=1}^{n} a_{(i)}^2}{n}} \tag{3}$$

where $\overline{a}_{\left(\frac{n+i}{2}\right)}$ is the calculated sliding root mean square (rms) of the acceleration signal corresponding to the $(n + i)/2$ sample of the acceleration signal; $a(i)$, the ith sample of the acceleration signal; n, the uneven number of samples used for the calculation of the rms.

The algorithm detects every time the rms exceeds the threshold and, in this segment, interpolates with a spline. Next, the polynomial function and the correction are automatically completed, obtaining the corrected deflection.

2.2 Viscoelastic material models

Asphalt concrete can be characterized as a material with viscous behaviour at high temperatures and/or slow loading rates. In order to model the asphalt concrete performance, a generalized Maxwell model can be utilized. Following the approach described in [9], it is assumed that volumetric pressure stress in the range of usual tire contact stresses causes elastic strain and relatively small time-dependent strain while deviatoric stresses are responsible for elastic as well as time-dependent strains [10]. The stress tensor decomposed into volumetric and shear components can be modelled as linear elastic and linear viscoelastic.

The linear viscoelastic behaviour can be represented by a generalized Maxwell model. Prony series are used to adjust the shear stress relaxation function of a viscous material, using Eq. 4.

$$G(t) = \sum_{k=1}^{K} G_k e^{-t/\tau_k} \tag{4}$$

where $G(t)$ is the calculated shear modulus at time t; τ_k, the parameters defining the relaxation times; G_k, the Prony coefficients; K, the number of elements of the generalized Maxwell model.

In the FE software Abaqus used in this work, the viscoelastic material is defined by a Prony series expansion of the dimensionless relaxation modulus [11]:

$$g_R(t) = 1 - \sum_{k=1}^{K} g_k (1 - e^{-t/\tau_k}) \tag{5}$$

where $g_R(t)$ is the dimensionless relaxation modulus; g_k and τ_k, the material parameters.

In the case of frequency dynamic data, the analytical expression can be deduced to convert the Prony series terms from time domain to frequency domain, using Fourier transforms:

$$G'(\omega) = G_0 \left(1 - \sum_{k=1}^{K} g_k\right) + G_0 \sum_{k=1}^{K} \frac{g_k \tau_k^2 \omega^2}{1 + \tau_k^2 \omega^2} \tag{6}$$

$$G''(\omega) = G_0 \sum_{k=1}^{K} \frac{g_k \tau_k \omega}{1 + \tau_k^2 \omega^2} \tag{7}$$

where $G'(\omega)$ is the storage shear modulus for frequency ω; $G''(\omega)$, the loss shear modulus for frequency ω; G_0, g_k, τ_k, the material parameters.

The model parameters G_0, g_k and τ_k can be obtained from frequency dependent test data, by minimizing the residual of the difference between the experimental and calculated shear storage and loss modules with an optimization algorithm. For CAST, the experimental complex shear modulus $G^*(\omega)$ can be calculated from the complex Youngs modulus $E^*(\omega)$ using Eq. 8:

$$G^*(\omega) = \frac{E^*(\omega)}{2(1 + \nu)} \tag{8}$$

where $G^*(\omega)$ is the complex shear modulus for frequency ω; $E^*(\omega)$, the complex Young modulus for frequency ω; ν, the Poisson ratio.

3 Experimental program

This section reports on the testing program and the characteristics of the testing sites. It also refers to the laboratory tests performed to obtain the mechanical properties of the pavement materials from the testing sites.

3.1 Full scale tests at the Circular Test Track

The Circular Test Track (CTT) is a full scale load simulator used for pavement research purposes, located in Dübendorf, Switzerland. The facility consists of five different pavement sections in a paved ring of 34 m diameter. The load is applied by three pinning arms which have ballasted dual tires at their ends. These tires can rotate at different speeds and change their loading position with time. This installation was equipped with several sensors like thermocouples, strain gauges and vertical deflectometers. However, only temperature was monitored during the present tests. Thermocouples were sensing temperature at a depth of −30 mm, −170 mm and −270 mm, for every pavement section. The static load of the double tires was 51.5 kN and the width of each single tire was 200 mm. There was a gap of 150 mm between them. The measured tire pressure was 0.7 MPa. A detailed description of the load simulator can be found in [12].

For the tests, an accelerometer was installed 40 mm beneath the pavement's surface in five sections of the CTT, in the centre line of the wheel track (unloaded area between the double tires). Measurements of acceleration induced by the rolling tires were carried out at two different traffic speeds, 20 km/h and 50 km/h. In this work, the results of two pavement sections depicted in Table 1 are discussed.

To determine the material parameters of the 1st and 2nd layers, cores were taken to carry out CAST, as explained later. The elastic modules of the 3rd and 4th layers were obtained with plate load tests carried out during the construction of the CTT pavement.

3.2 Road tests at the A1 motorway

Further tests were carried out in a monitoring site along the A1 motorway that connects Zurich with Bern, in Switzerland [15]. Table 2 displays the geometry and material of the full depth structure classified according to [13].

The material properties were obtained in the laboratory with CAST, as described in next section. The elastic modulus of the subgrade was also measured using a Light Drop-Weight tester (LDW), after extraction of a pavement block down to the subgrade depth. For the tests, nine accelerometers were installed 40 mm below the pavement surface. The sensors were positioned in a triangular array to

Table 2 Thickness and materials of the pavement layers of the A1 motorway

Layer	Thickness	Material
1st	40 mm	SMA 11S[a]
2nd	70 mm	AC T 22H[b]
3rd	120 mm	AC T 32H[c]
4th	95 mm	AC F 22S[d]

[a] Stone mastic asphalt for heavy traffic, maximum aggregate size 11 mm

[b] Low deformation, asphalt concrete base course for heavy traffic, maximum aggregate size 22 mm

[c] Low deformation, asphalt concrete base course for heavy traffic, maximum aggregate size 32 mm

[d] Asphalt concrete subbase course for heavy traffic, maximum aggregate size 22 mm

Table 1 Geometry and materials of two sections of CTT (F1 and F2)

Layer	Thickness	Materials—Field 1	Materials—Field 2
1st	40 mm	Asphalt concrete 11 max aggregate	
2nd	140 mm	Crushed fluvial gravel, binder 50/70	Crushed fluvial gravel, special binder EME2
3rd	320 mm	Crushed gravel sand	
4th	1,500 mm	Silt sand	

EME2 stands for "enrobé à module élevé class 2", as described in [13, 14]

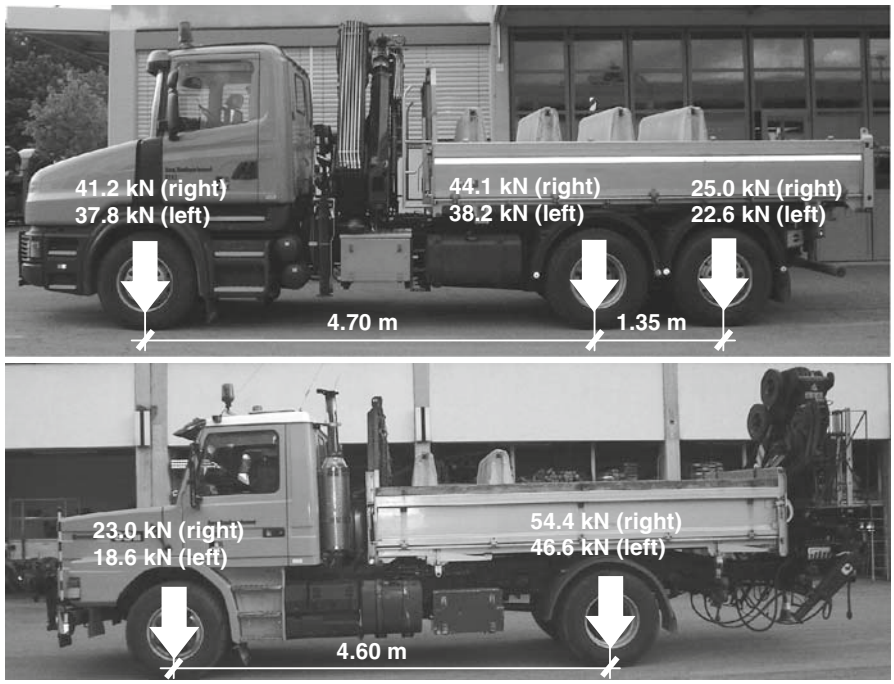

Fig. 1 Geometry and loads of the (**a**) three axle and (**b**) two axle trucks used for the A1 motorway tests. The side of the truck where the load is applied is given in brackets

obtain the deflection basin of the entire truck and check for the longitudinal repeatability of the results. Two trucks with two and three axles were driven over the site at speeds of 20 km/h, 50 km/h and 70 km/h. The geometry and static loads of the vehicles is presented in Fig. 1. During the tests, pressure distributions of the footprints of the tires were measured using the Stress in Motion MODULAS Kistler sensor [16]. This sensor consists of a linear array of piezoelectric sensors of 15 mm width and 50 mm length installed flush with the pavement surface that gives the discrete tire load while the tire rolls over the sensor. Speed, geometry and total load of the vehicles were monitored by the piezoelectric Weight in Motion (WIM) LINEAS Kistler sensor. Climate parameters such as temperature and moisture were monitored throughout the depth of the pavement. Additionally, the response of the structure under load was measured by a set of three magnetostrictive deflectometers installed in a line perpendicular to the direction of the vehicle movement, matching the positions of the accelerometers. These sensors measured the differential vertical deformations at three depths of the structure relative to the base cap, positioned 40 mm beneath the pavement surface. Only the relative deformation between the base cap and the deepest monitor location positioned 640 mm below the surface (i.e. 315 mm into the subgrade) were considered in the present analysis.

Static tests were carried out to validate the FE models. These tests consisted of applying the constant load of the right rear tire of the two axle truck upon one of the deflectometers and measuring the deflection curve over 15 min.

3.3 Material properties

The mechanical properties of the asphalt concrete layers were determined with CAST. These tests provide the complex modulus and phase angle of the materials at different temperatures and load frequencies by applying sinusoidal loads in the inner part of a ring shaped specimen. The deformation of the internal diameter of the specimen is measured with a LVDT. The elastic modulus is then obtained based on FE calculations [6]. In this work, the material properties of the asphalt concrete layers were modelled using temperature and frequency dependent elastic and linear viscoelastic constitutive laws. The complex modulus was obtained for temperatures between −10°C and 30°C and for frequencies from 0.250 Hz to 16 Hz. Experimental data obtained from these tests were used to calculate master curves for each material at a reference temperature of 20°C

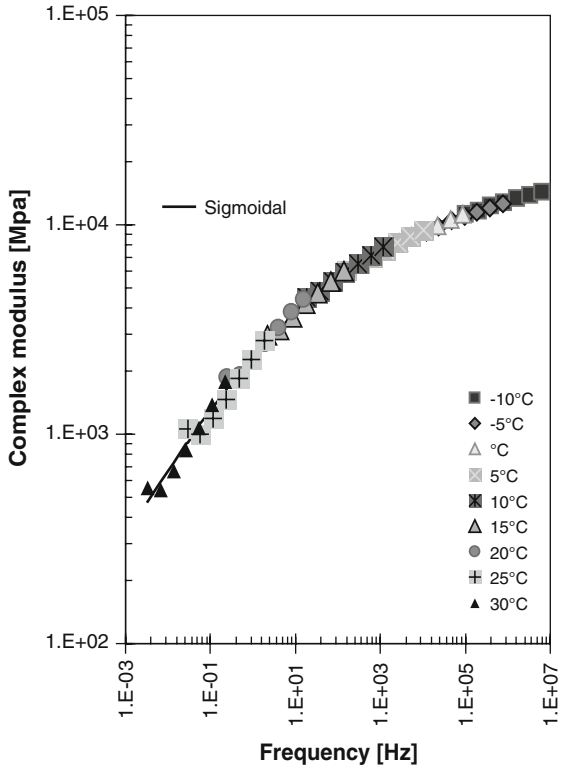

Fig. 2 Example of the sigmoidal model curve at 20°C for layer 4 (HMT22) of A1 motorway, obtained from CAST tests

considering the Williams-Landel-Ferry (WLF) time-frequency superposition principle and a sigmoidal approach [17] (Fig. 2). The viscoelastic material parameters G_0, g_k and τ_k were deducted from CAST as explained before. The granular and subgrade layers of the pavements were considered as linear elastic materials, and their values were determined in situ.

4 Finite element analysis

In order to conduct a theoretical analysis of the deflections obtained in the experimental phase, different viscoelastic FE models were created. The models provided the only way to study the deflections obtained at the CTT since in this pavement section no deflectometer was used during the tests. The software Abaqus 6.5 was chosen to create the models. A plug-in with Python scripting language was developed in order to allow systematic analysis by changing the variables involved in typical pavement facilities, namely pavement geometry (size of the modelled part, number of layers and layers thicknesses), material properties, temperature, loading conditions, etc. Two models were created:

- *Static model*. Reproduced the deflection of a pavement loaded with a non moving tire. It was used to simulate static tests on the A1 motorway. In this model the dynamic effect of a rolling tire was neglected. Due to its simplicity it was utilized to verify the accuracy of the material properties obtained in laboratory and field tests.
- *Dynamic model*. Had the same geometry and material properties as the static model but considered the inertial effects produced by the dynamic loading of moving trucks. It was used to make a qualitative and quantitative comparison to the measured deflections of the dynamic tests of the A1 motorway and the CTT.

4.1 Static model

This model was developed taking into account the geometry of the pavement of the A1 motorway. The size of the modelled section was 4,000 mm by 4,500 mm. These dimensions were chosen to reduce the effect of the boundary conditions on the size and shape of the deflection bowl. The depth of each layer of the model was set as an average value of the pavement layer thicknesses. The subgrade was modelled as an elastic layer 1,650 mm thick. Adding all layers, the height of the model was 1,975 mm (Fig. 3). The material properties of each layer were stored in a material library. The asphalt concrete layers were modelled using viscoelastic constitutive laws deducted from CAST. Master curves were obtained using the WLF equation and the sigmoidal approach. Temperature dependency was considered for each layer, but not for the subgrade. For all layers, reduced integration eight nodded elements C3D8R were used. The sizes of the elements in the different layers varied from the top to the bottom. In the area of the tire footpath, the elements size was similar to the size of the channels of the MODULAS sensor (15 mm × 50 mm). Outside this area and in the layers below, a coarser mesh was used. Regarding the boundary conditions, the elements at the bottom surface were fixed in all directions while the four lateral sides were symmetrically fixed. The tire load was represented by constant pressure functions

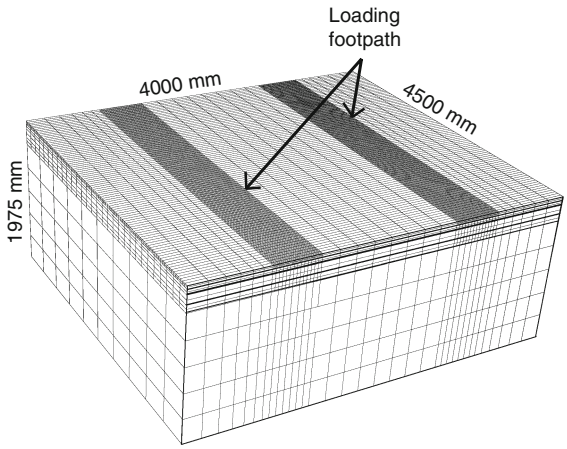

Fig. 3 Geometry of the FE model used to simulate the tests at the A1 motorway

applied on the elements of the surface, over a period of time equivalent to the duration of the test. The amplitudes of the pressure functions were deducted from the MODULAS stress in motion measurements. Although MODULAS measures the average time pressure distribution of a moving tire, this can be converted to an average tire static pressure by multiplying the time dependent pressure times the truck speed measured by the LINEAS sensor (Fig. 4). Then, the average pressure applied in the area of a MODULAS channel is used as the input pressure applied on the surface element. Therefore the exact geometry of the loading area and the pertinent pressure conditions on each tire tread were considered in the model. Abaqus Standard solver was chosen for the calculation. The viscous option was enabled to consider the viscoelastic characteristics of the materials to obtain the entire time history of the deflection.

4.2 Dynamic model

The geometry and material properties used in the motorway dynamic model were the same as in the static model. However, in this case the rolling of the tire over the model was simulated shifting the pressure functions stepwise along each element of the model footpath with the same speed as the simulated vehicle. The time used in each step was equal to the length of the element (50 mm) divided by the speed of the vehicle. The model was solved every time the pressure function achieved the full passage of one element. To consider the dynamic nature of the event, Abaqus Explicit was used as solver.

The dynamic model was used to simulate the CTT tests, changing the geometry of the model according to the geometry of the CTT. Thus, the modelled piece had 5,000 mm long, 4,500 mm wide and four layers in depth. The material parameters of the two upper layers where determined with CAST. The granular materials of the bottom of the structure where modelled as linear elastic. For these tests the pressure distribution of the tires was unknown. Next, the total load of the tire was distributed over a rectangular footprint of 200 mm × 189 mm giving a uniform pressure of 0.7 MPa. The load footprint was moved over the surface of the model in a similar way as in the model of the motorway, and a similar meshing was used.

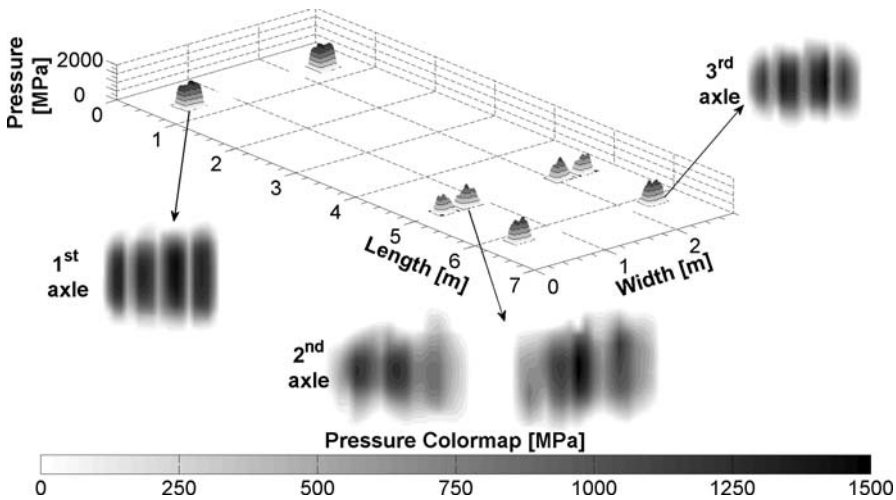

Fig. 4 Three dimensional view of the footprint of a three axle truck measured with MODULAS and a two dimensional pressure distribution colour map of each tire

5 Results and analysis

Figure 5a–c presents the results obtained in the A1 motorway for a vehicle of three axles travelling at 20 km/h, 50 km/h and 70 km/h, respectively. The straight lines represent the measured relative deflections between two positions 40 mm and 640 mm below the surface, obtained with the magnetostrictive deflectometers. The dashed lines correspond to the calculated deflections, deduced from acceleration measurements. Based on the qualitative comparison of both deflections plots, the following findings can be drawn:

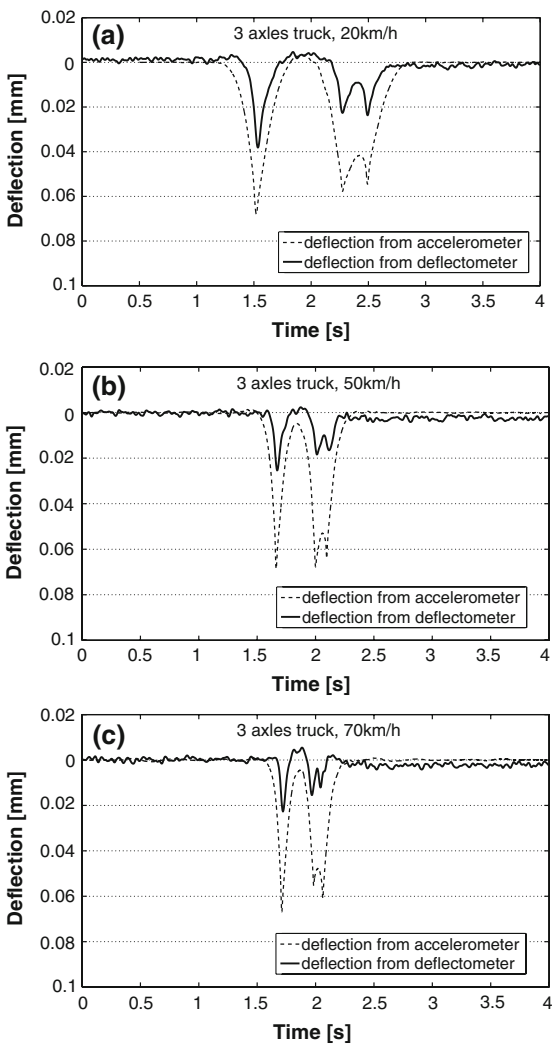

Fig. 5 Three axle truck moving at (**a**) 20 km/h, (**b**) 50 km/h and (**c**) 70 km/h

- The measured and calculated deflection peaks produced by each of the three axles of the truck exhibit a perfect correlation in time. This holds true for each testing speed.
- The analysis of the amplitudes shows that the calculated deflection is always larger than the measured deflection. This divergence can be partly explained because, as mentioned in the introduction, accelerometers measure the deflection of the entire pavement structure while deflectometers measure only deflections relative to a reference point. Although this is consistent with the expected results, it is not possible to establish with accuracy if a portion of the differences are due to errors of the method proposed in this work.
- For all the cases, the deflection produced by the front axle (1st peak) is larger than the ones produced by the rear axles (2nd and 3rd peaks). Still, the difference is more evident in case of the deflectometer and not very clear for the accelerometer. One probable explanation is that 2nd and 3rd axles produce a large deflection area far below in the subgrade, superimposing all deflections as if they were produced by a single axle. The addition of deflections of the 2nd and 3rd axles was measured by the accelerometer but not by the deflectometer and this is reflected in the order of magnitude of the peaks.
- A similar effect is produced by the speed of the vehicle. The faster the vehicle, the smaller the deflection measured by the deflectometer. This might be caused by the fact that the modulus of the asphalt concrete depends of the loading rate: the higher the frequency, the higher the modulus and the smaller the deformation. As the subgrade is composed of unbound materials, the loading speed does not have a significant effect on the material elastic modulus, and therefore on the deformation. Thus, the influence of the vehicle speed on the total deflection is relatively negligible when measured with the accelerometer, as it also includes the deflection of the subgrade.
- Between the two peaks produced by the front and rear axles, the deflectometer results show that the pavement suffers a tensile deformation in the vertical direction. This effect is not registered by the accelerometer, since it measures the total deflection of the structure that is compressive in average.

Similar results as the previously reported were obtained for the two axle truck used in the tests. As an example, Fig. 6 presents the measured and calculated deflections induced by the vehicle travelling at 50 km/h.

With multiple sensors arrays it was possible to create three dimensional deflection maps of moving trucks. Figure 7 shows the deflection of a 10 m × 2.5 m pavement portion when two (a) and a three (b) axle trucks are travelling at 50 km/h. The plots were made using the set of three deflectometers installed in the A1 motorway. For the same trucks and speeds, deflection maps measured with accelerometers are depicted in Fig. 8. The vertical deformation of both Figs. 7 and 8 are given in the same scale for better comparison. A qualitative analysis of the results showed that deflections obtained from deflectometers and from accelerometers arrays have the same shapes, but the latter exhibits larger amplitudes. This is in accordance with the expected results. However, it was found that for slowly moving trucks (20 km/h) it was not possible to construct deflection maps. This is because the calculation algorithm didn't work accurately for accelerometers positioned far away from the tire load. At those locations the registered accelerations were too weak.

In the static tests, pavement deformation was measured over several minutes with one of the magnetostrictive deflectometers. After 800 s the results showed a deflection of 0.27 mm. Results of the initial static FE model showed however, that the simulated deflection was 0.39 mm. One probable

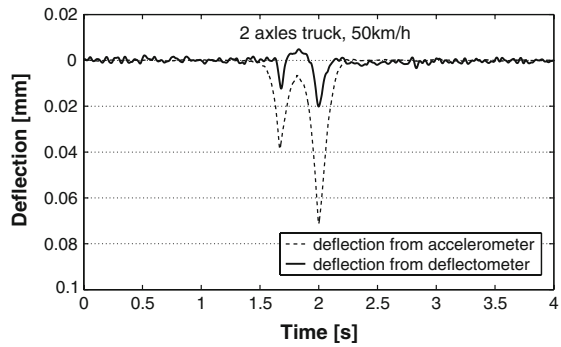

Fig. 6 Two axle truck moving at 50 km/h

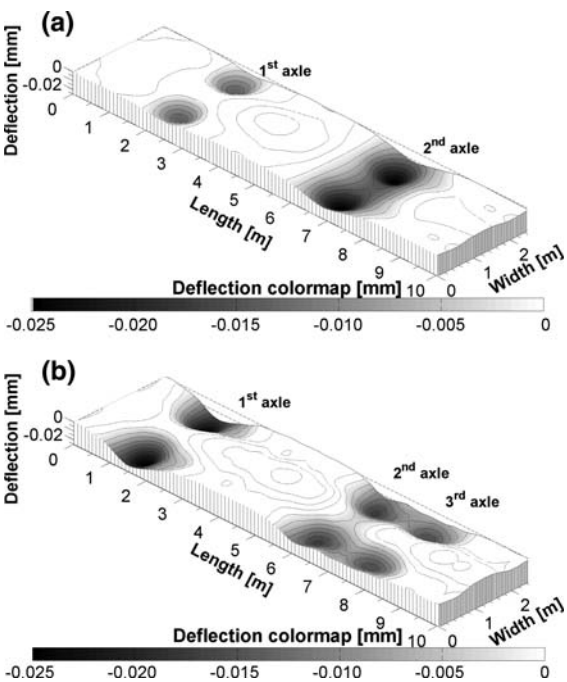

Fig. 7 Three dimensional deflection maps of a (**a**) two axle and (**b**) three axle truck moving at 50 km/h, measured with deflectometers. The lines show equal deflection contours every 0.0025 mm

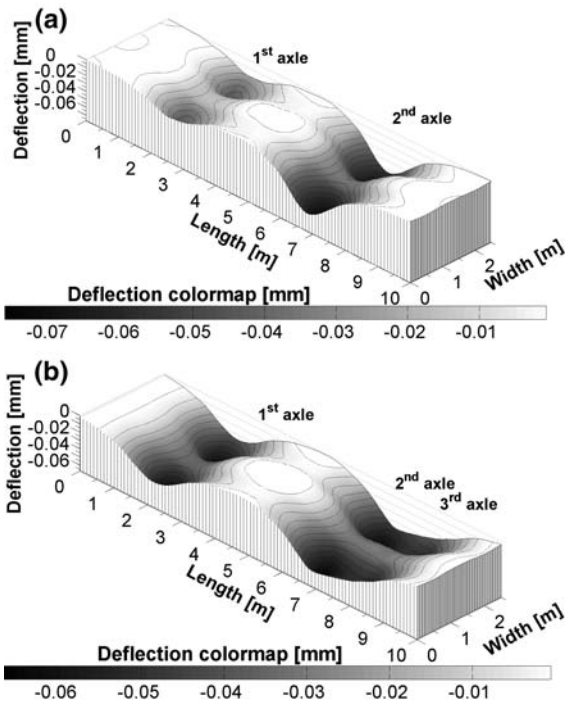

Fig. 8 Three dimensional deflection maps of a (**a**) two axle and (**b**) three axle truck moving at 50 km/h, measured with accelerometers. The lines show equal deflection contours every 0.005 mm

origin of this incongruity was the use of an incorrect subgrade modulus in the FE model, which was obtained with a Light Drop Weight (LDW) tester. To do the tests it was necessary to open a pit to reach the testing surface. It is believed the water used in the pavement cutting filtered and affected the subgrade and therefore influenced the LDW results. In addition, it is suspected that the subgrade modulus was also affected by the lack of confining pressure given by the missing material of the pit. Consequently, the elastic modulus of the subgrade was corrected, increasing it for a factor of 1.5 (from 140 MPa to 210 MPa) until the measured and modelled deflection showed a good match, as shown in Fig. 9. This new subgrade modulus was believed to more accurately represent the real modulus and therefore was used in the dynamic FE model.

Figures 10 and 11 show the results of the dynamic FE models, simulating the passing at 50 km/h of a three and a two axle truck over the motorway surface compared to the deflection produced by the same vehicles, calculated from acceleration measurements. A qualitative analysis of the shapes shows simultaneous peaks and similar deflection amplitudes. The modelled deflection, however, tends to show a faster recovery after the load release and therefore the model presents smaller deflection bowls than those calculated from acceleration. This is probably due to the fact that models are finite although pavements are a semi-infinite media. The fixed boundary conditions of the edges of the model restrict and confine the deflection area to the limits of the model, restraining their amplitude and shape. In addition, the endless subgrade is actually modelled as a finite layer. Additionally, the distribution of the pressure on the subgrade is limited by the depth of the model whereas in the reality the load is distributed in a larger area.

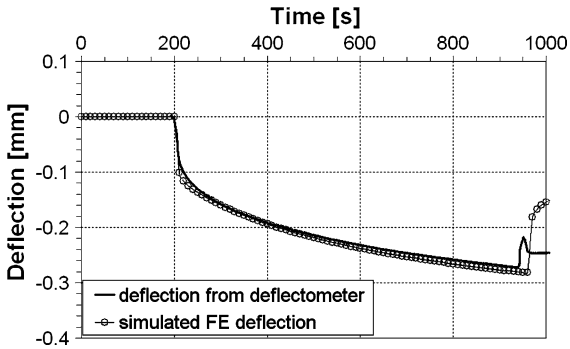

Fig. 9 Comparison between static pavement deflections measured with deflectometer and calculated with the FE static model

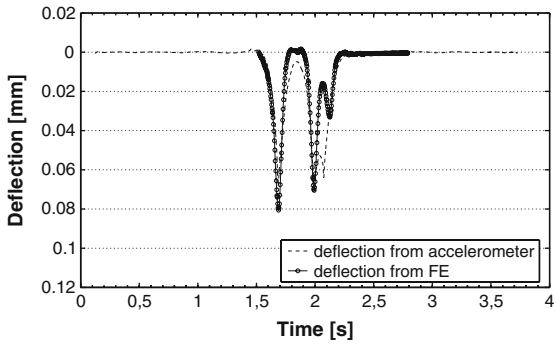

Fig. 10 Comparison of the acceleration derived deflections and dynamic FE model deflections for a three axle truck at 50 km/h

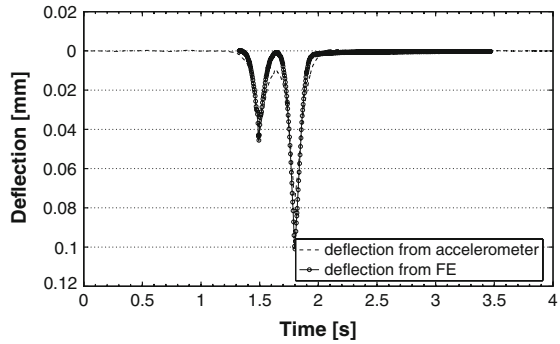

Fig. 11 Comparison of the acceleration derived deflections and dynamic FE model deflections for a two axle truck at 50 km/h

The deflections obtained by the accelerometers installed in the CTT presented amplitudes of less than a half of those obtained with the dynamic FE model. This difference is most likely due to the conditions in which the tests to estimate elastic modulus of the unbound layers were carried out. The plate load tests were done during the construction of the pavement. The compaction work of the upper layers and the progressive compaction of all the layers due to millions of tire loads (the CTT was used as a long term testing facility), increased the modulus of the layers underneath over time. Additionally, the elastic modules of the unbound layers used in the firsts FE simulations were actually underestimated. An increase of the values

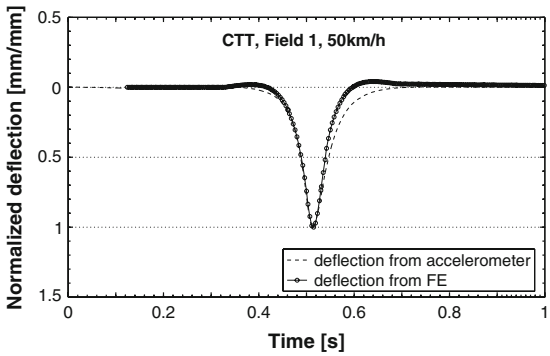

Fig. 12 Normalized deflections from accelerometers and simulated with the dynamic FE model of the CTT, Field 1, for a testing speed of 50 km/h

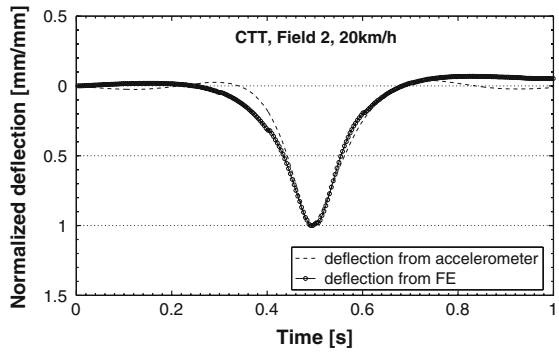

Fig. 13 Normalized deflections from accelerometers and simulated with the dynamic FE model of the CTT, Field 2, for a testing speed of 20 km/h

in the order of two times provided similar deflections in the model as in those calculated from accelerations. In order to complete a qualitative comparison between the modelled and the calculated deflections time histories, both records were normalised to the maximum amplitude. Figure 12 presents the normalised deflections of Field 1 for a tire moving at 50 km/h. The shapes again show a faster recovery for the deflection of the model. However, the differences between the deflection shapes are not as pronounced as for the motorway dynamic model. The boundary conditions of the CTT dynamic model have less influence on the deflection shapes for two reasons:

- In the CTT model only one tire load is modelled. Hence, the distance from the load to the model borders is relatively larger than for the motorway model.
- The pavement structure of the CTT load simulator was built inside a trapezoidal pre-stressed concrete cast. The fixed boundaries of the dynamic model represent more accurately the behaviour of a rigid concrete frame.

Additional differences can be detected just before and after the tire passing. The model reveals vertical tensile strains tending to return to the original position very slowly (delayed recovery), because of the viscous nature of the asphalt concrete. This trend is even more pronounced at lower speeds as can be seen in Fig. 13. The differences between the deflection shapes might be due to the difficulty of the accelerometer to accurately measure low frequency motion.

6 Conclusions

This study shows that pavement elastic deflection produced by moving vehicles can be estimated with a method that uses accelerometers and a correction algorithm. Results should be considered with caution however, since no precise quantification of potential errors was carried out. Additionally, it was found the method does not work when the intensity of the induced accelerations is weak. Slowly moving, light loaded vehicles passing far away from the sensor position represent unfavourable conditions for the use of accelerometers. Moreover, as demonstrated with the FE models, quasi-static or very slow pavement motions like the viscoelastic delayed recovery of asphalt concrete, are not measured by the accelerometer. Nevertheless, for typical truck speeds and loads, the method proved capable of measuring elastic deflections of the entire structure that are reasonable, with relatively low installation effort, time and cost. Examples of the potential of the method are the deflection maps presented in the paper, obtained with the installation of a set of multiple accelerometers. In a future work, mounting of accelerometers at different depths and subtracting the deflection of each level would allow plotting relative deflection maps similar to those made with the magnetostrictive deflectometers.

References

1. De Beer M, Horak E, Visser AT (1989) The multidepth deflectometer (MDD) system for determining the effective elastic modules of pavement layers. In: Bush AJ III, Baladi

GY (eds) Nondestructive testing of pavements and back calculation of modules, ASTM STP 1026. American Society for Testing and Materials, Philadelphia, pp 70–89
2. Tabatabaee N, Al-Quadi IL, Sebaaly PE (1992) Field evaluation of pavement instrumentation methods. J Test Eval 20(2):144–151
3. Raab C, Partl MN, Anderegg P, Brönnimann R (2003) Two years experience with a new long-term pavement performance monitoring station on a Swiss motorway. In: Proceedings of 3rd international symposium on maintenance and rehabilitation of pavements and technological control, 7–10 July, Minho University, Guimarães, Portugal, pp 263–271
4. Hoffman MS, Thompson MR (1982) Comparative study of selected nondestructive testing devices. Transp Res Rec 852:32–41
5. Tandon V, Nazarian S (1992) Comprehensive evaluation of five sensors used to measure pavement deflection. Transp Res Rec 1355:27–36
6. Sokolov K, Gubler R, Partl MN (2005) Extended numerical modeling and application of the coaxial shear test for asphalt pavements. J Mater Struct 279:515–522
7. Arraigada M, Partl MN, Angelone SM (2007) Determination of road deflections from traffic induced accelerations. Road Mater Pavement Des 8(3):399–421. doi:10.3166/rmpd.8.399-421
8. Boore DM (1999) Effect of baseline corrections on response spectra for two recordings of the 1999 Chi-Chi, Taiwan, Earthquake. U.S. Geological Survey Open File Report 99–945. U.S. Geological Survey, 1999
9. Blab R, Harvey JT (2002) Modeling measured 3D tire contact stresses in a viscoelastic FE pavement model. Int J Geomech 2(3):271–290. doi:10.1061/(ASCE)1532-3641(2002)2:3(271)
10. Collop AC, McDowell GR, Lee YW (2006) Modelling dilation in an idealised asphalt mixture using discrete element modelling. Granul Matter 8:175–184. doi:10.1007/s10035-006-0013-3
11. ABAQUS Version 6.5 Documentation (2004) ABAQUS Inc.
12. Caprez M, Rabaiotti C (2006) Review and future perspective of road research in Switzerland based on "Rundlauf'' Circular Test Track results. In: Baoshan H, Roger M, Jorge P, Erol T (eds) Proceedings of sessions of GeoShanghai 2006, ASCE, pp 134–141
13. Swiss Standard SN 640 430b (2008) Walzasphalt. Ausführung und Anforderungen an die eingebauten Schichten. (Hot rolled asphalt. Construction and requirements of the pavement layers) Schweizerischer Verband der Strassen- und Verkehrsfachleute VSS
14. Swiss Standard SN 640 431-1b-NA (2008) Asphaltmischgut Mischgutanforderungen—Teil 1: Asphaltbeton. (Asphalt mix requirements—part 1: asphalt concrete) Schweizerischer Verband der Strassen- und Verkehrsfachleute VSS
15. Poulikakos L, Heutschi K, Anderegg P, Calderara R, Doupal E, Siegrist R et al (2005) Determination of the environmental footprint of Freight vehicles. In: Proceedings of 4th international conference on weigh-in-motion ICWIM4, 20–22 Feb, Taipei, Taiwan, pp 189–197
16. Doupal E, Gysi M (2002) Measurement of dynamic wheel load distributions. In: Proceedings of NATMEC 2002—ICWIM-3 Congress, Orlando, FL, USA, May 13–15
17. Pellinen TK, Witczak MW (2002) Stress dependent master curve construction for dynamic (complex) modulus. Annual meeting association of asphalt paving technologists, Colorado Springs, Colorado, USA